Dynamics of Excimer Formation and Relaxation in the T-Shaped Benzene Dimer

Toshihiko Hirata, Hiroshi Ikeda, and Hiroyuki Saigusa*

Department of Environmental Sciences, Graduate School of Integrated Sciences, Yokohama City University, Yokohama 236, Japan

Received: September 22, 1998

The excited-state dynamics of the T-shaped van der Waals (vdW) dimer of benzene has been studied by probing fluorescence after S_1 excitation. Excimer fluorescence is observed when the dimer is excited into the S_1 origin and the ν_6 vibronic level. The results demonstrate that the excimer formation proceeds by tunneling through an energy barrier between vdW and excimer potential wells. Use of a pump−probe fluorescence depletion technique showed that the excimer absorbs strongly at 500 nm, consistent with the result in solution. Evidence is observed for an equilibrium between the vdW dimer and excimer states in the ν_6 excitation. These results are explained by invoking an excimer of a parallel stacked geometry, having a charge-transfer character. The excimer formation dynamics of the benzene dimer is discussed based on comparison with those of other aromatic dimers and cluster systems.

I. Introduction

The benzene dimer represents one of the few examples of aromatic dimers whose geometrical structures have been the subject of various experimental and theoretical studies. It is important primarily because the benzene−benzene interaction may be considered as a model for studying the intermolecular interaction in aromatic systems. Recent experimental results of Raman-vibronic double-resonance spectroscopy[1] and of Fourier transform microwave spectroscopy[2] have converged on a T-shaped geometry in which one benzene moiety is located at the top of the T and the other moiety at the stem. This dimer structure suggests that two benzene moieties are highly fluctuant and freely rotating along the axis connecting the mass centers of the monomers. Although results of quantum chemical calculations still remain controversial,[3−8] the experimentally observed T-shape scenario has been firmly established for the ground-state dimer.

However, structural and dynamic information about the electronically excited benzene dimer has been elusive. Hopkins et al.[9] used a mass-selective two-color photoionization method to measure the dynamics of the S_1 dimer. From the shortening of the S_1 lifetime with respect to the monomer, they suggested that the dimer transforms into an excimer geometry having two benzene planes parallel and closely spaced. They also reported an efficient two-color ionization yield from the S_1 intermediate levels. Similar photoionization results were obtained by Law et al.[10] Subsequently, Langridge-Smith et al.[11] attempted to measure laser-induced fluorescence signals from the dimer and found that its fluorescence yield is abnormally low. More recently, stimulated emission pumping experiments have been carried out for S_1 benzene clusters by Krätzschmar et al.[12] The absence of any signals for the dimer has been ascribed to a floppy structure of this species.

For the S_2 state of the benzene dimer, Shinohara and Nishi[13] measured its lifetime using pump−probe photoionization spectroscopy, from which they concluded that the dimer undergoes excimer formation on the nanosecond time scale. However, Ernstberger[14] failed to reproduce this experiment. The S_2 lifetimes have recently been reexamined by Radloff et al.[15] with femtosecond pump−probe methods. The short lifetime of the dimer (40 fs) has been attributed to a rapid internal conversion into the S_0 state.

The occurrence of excimer formation has been demonstrated for various dimers and clusters of large aromatic molecules in a molecular beam.[16] For example, the fluorene ($C_{13}H_{10}$) dimer produces exclusively excimer fluorescence after excitation into the S_1 state of the vdW potential.[17,18] Unfortunately, spectroscopic data for these systems are not sufficient to determine their geometries uniquely. The benzene dimer is therefore of considerable importance in elucidating the relationship between the structure and excited-state dynamics because its vdW geometry is established to be T-shaped.

In the present work we concentrate on the excited-state dynamics of the T-shaped benzene dimer and show that it undergoes geometry changes to the tightly bound excimer upon excitation into the S_1 state. We observe excimer fluorescence after excitation into the electronic origin (0^0) and ν_6 (6^1) vibronic level. Previously, the fluorescence of the benzene excimer was observed only in a highly concentrated solution (>1 M), with an intensity maximum at ≈315 nm.[19] Using a pump−probe photodepletion technique, we show that the benzene excimer formed from the S_1 vdW dimer absorbs strongly at ≈500 nm. The structure and dynamics of the excimer are discussed based on these results, and compared with those of other aromatic systems.

II. Experimental Section

Fluorescence excitation, dispersed fluorescence, and fluorescence decay measurements were carried out on supersonically cooled benzene clusters. Clusters were generated by passing helium at 3 atm over liquid benzene at 0 °C, and expanding through a pulsed valve (General Valve). The beam interacted at 10 mm downstream with the doubled output (7 ns) of a YAG-pumped dye laser (Continuum PL8000/ND6000/UVT-1). Fluorescence was collected either by a filter or a 0.32-m monochromator (Jobin-Yvon HR320), and detected with a PMT

10.1021/jp983814z CCC: $18.00
Published on Web 02/06/1999

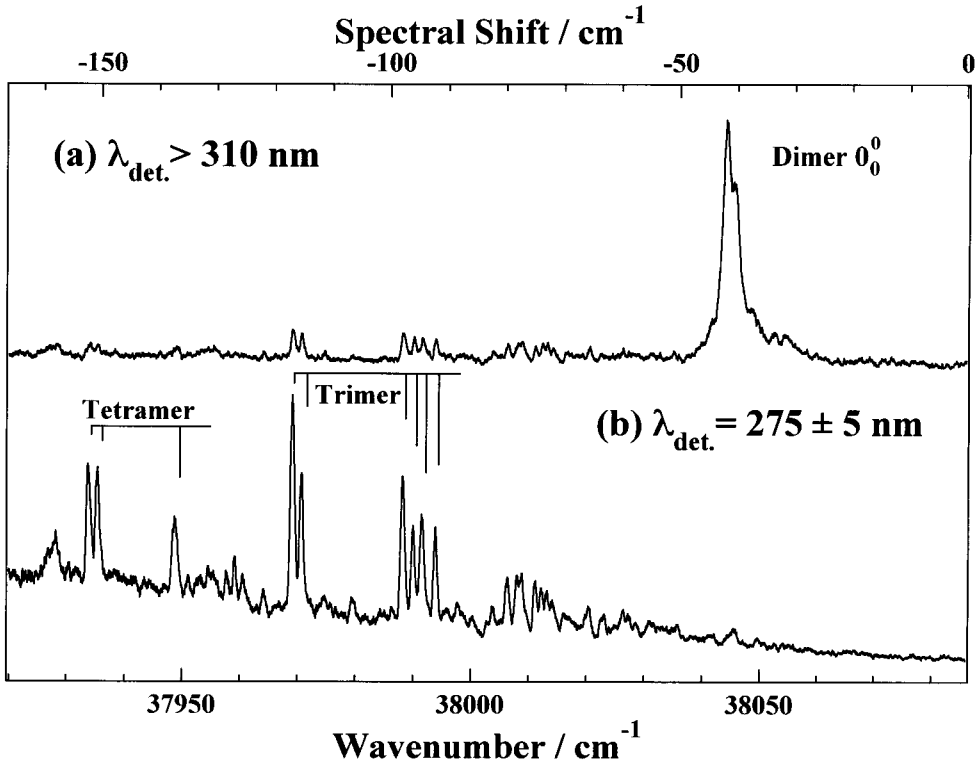

Figure 1. Fluorescence excitation spectra of the pure benzene clusters in the S_1 origin region, obtained by detecting fluorescence (a) at >310 nm and (b) at 275 ± 5 nm. The spectral shift is relative to the monomer origin at 38 086 cm^{-1}.

(Hamamatsu R928). The PMT output was averaged with a boxcar integrator or time-resolved with a fast oscilloscope, and then sent to a computer for analysis.

In photodepletion experiments, part of the frequency-tripled output of the YAG laser was used to pump a second dye laser (Molectron DL-14). The visible (probe) beam was delayed by ≈7 ns with respect to the pump beam. The pulse energy of the pump beam at the sample was 0.1 mJ, whereas that of the probe beam was varied in the range 0.1−0.5 mJ (typically 0.35 mJ). The pump beam was focused to produce a beam diameter of 1−2 mm, with the probe beam being less tightly focused (≈5 mm), to ensure that the probe beam interacted with all species excited with the pump beam. Temporal profiles of the photodepletion experiments were obtained by subtracting the fluorescence decay curve with the pump laser alone from that with the probe laser on. No fluorescence was detected with the probe laser alone.

Fluorescence measurements were also carried out on pure and mixed dimer isotopomers of benzene, $(C_6D_6)_2$ and (C_6H_6)-(C_6D_6). A 1:1 preexpansion mixture of C_6H_6 and C_6D_6 was used to generate the mixed dimer isotopomer.

III. Results

A. Fluorescence Excitation Spectra. The fluorescence excitation spectra of small benzene clusters in the S_1 origin and 6_0^1 band regions were reported by Langridge-Smith et al.[11] The spectra exhibited very weak features corresponding to the dimer, from which they concluded that the dimer fluorescence yield is anomalously low. This result, when combined with apparently unexplained ionization results, strongly suggests that the excimer forms after excitation in these regions, thus emitting weakly at the initially excited T-shaped geometry. Because the fluorescence of the excimer in solution is shifted considerably from that of the monomer,[19] we record fluorescence excitation spectra by collecting exclusively monomer-like fluorescence at 275 ± 5 nm or red-shifted excimer fluorescence at >310 nm by the procedure described in section II. Figure 1 shows the excitation spectra in the S_1 origin region. The dimer 0_0^0 feature appears only in the excimer fluorescence spectrum of Figure 1a. The spectral shift is −42 cm^{-1} with respect to the monomer origin. Note also the splitting of the band, which matches the splitting (1.4 cm^{-1}) observed by Börnsen et al.[20] using mass-selective spectroscopy. With the detection wavelength set to 275 nm, no corresponding peak is observed (Figure 1b). In contrast, peaks that can be assigned to the trimer and tetramer are seen in this spectrum. The broad background whose intensity increases toward the lower energy region is assigned as arising from excitation of larger clusters than the tetramer. It is also important to note that the dimer feature appears to be broader than those of the trimer and tetramer.

Figure 2 shows the excitation spectra in the 6_0^1 region. The dimer 6_0^1 (0_0^0 + 521 cm^{-1}) transition appearing in the excimer excitation spectrum of Figure 2a gives rise to a doublet corresponding to excitation of the stem site of the T-shaped structure, which is followed by vdW progression(s) caused by excitation of the top site.[1] The intensity ratio (3:2) of the doublet at −43 and −40 cm^{-1} with respect to the monomer 6_0^1 band agrees well with that observed using mass-selective ionization spectroscopy.[9,10] Both the doublet structure and the vdW progression(s) are also present (albeit very weak with respect to the trimer features) in the excitation spectrum of 275 nm fluorescence (Figure 2b). This behavior indicates that both vdW and excimer fluorescence are produced after 6_0^1 excitation. Unfortunately, the monomer 16_0^2 (474 cm^{-1}) transition and the red-most peak of the dimer nearly coincide.[10,21] Therefore, the −43 cm^{-1} peak that appears in the spectrum detected at 275 nm (Figure 2b) is assigned as a superposition of the dimer 6_0^1 and monomer 16_0^2 transitions.

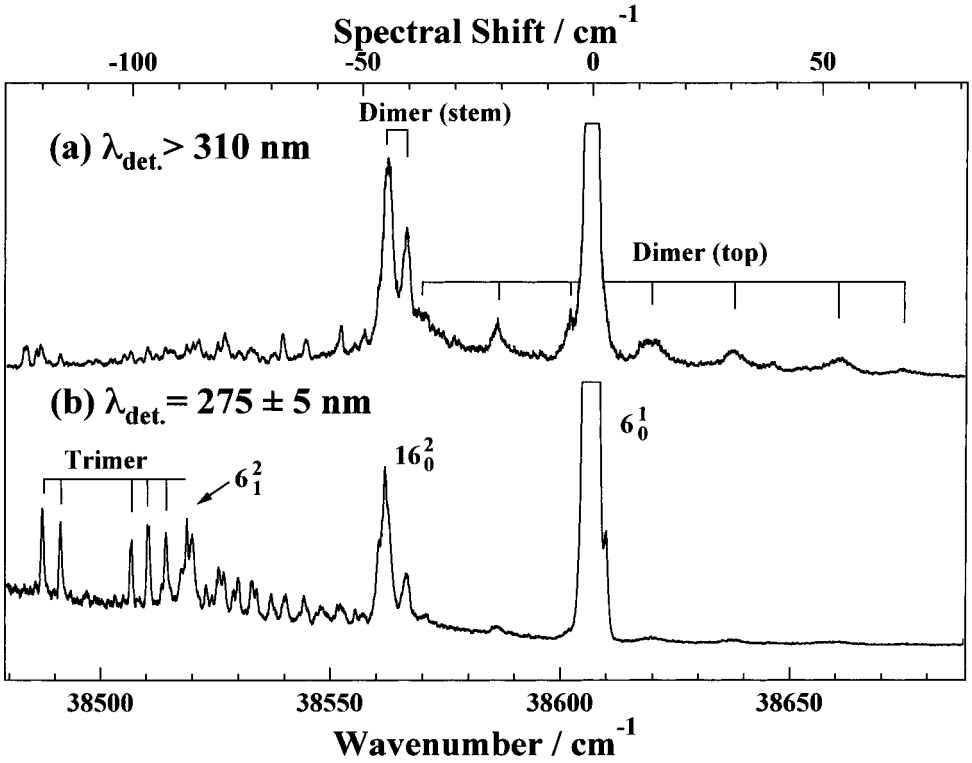

Figure 2. Fluorescence excitation spectra of the benzene clusters in the 6_0^1 region, obtained by detecting fluorescence (a) at >310 nm and (b) at 275 ± 5 nm. The spectral shift is relative to the monomer 6_0^1 transition at 38 608 cm^{-1}.

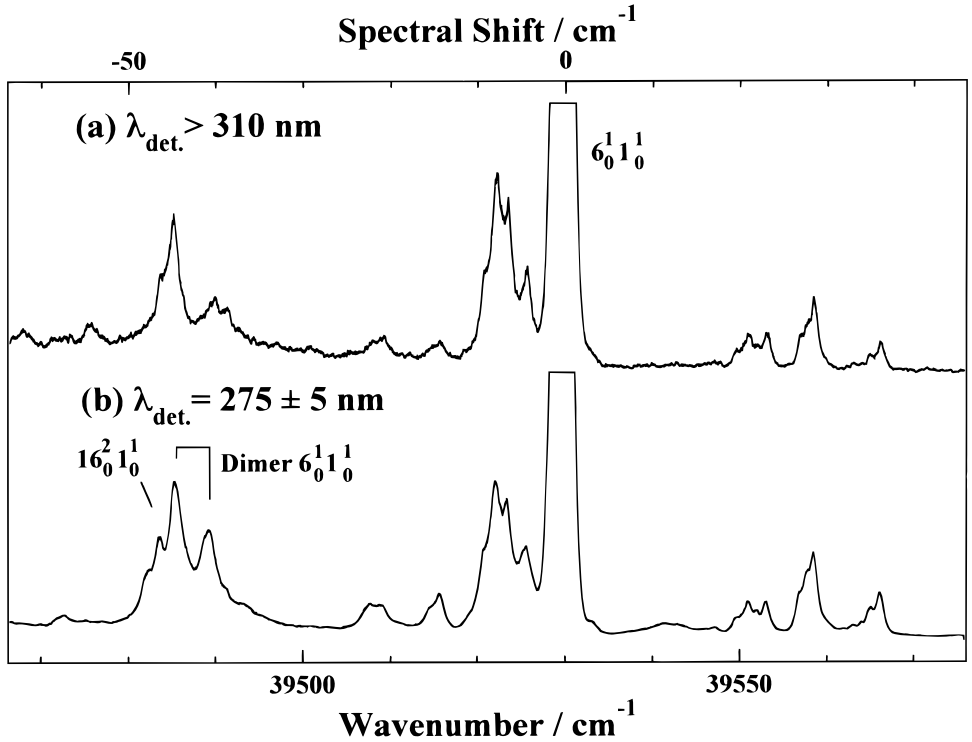

Figure 3. Fluorescence excitation spectra of the benzene clusters in the $6_0^1 1_0^1$ region, obtained by detecting fluorescence (a) at >310 nm and (b) at 275 ± 5 nm. The spectral shift is relative to the corresponding monomer transition at 39 531 cm^{-1}.

Figure 3 shows the excitation spectra in the region of $6_0^1 1_0^1$ (0_0^0 + 1444 cm^{-1}), which were obtained by detecting monomer-like fluorescence and excimer fluorescence. The doublet structure that appears at −43 and −40 cm^{-1} with respect to the monomer $6_0^1 1_0^1$ is assigned to the stem of the dimer. Analogous to the situation in the 6_0^1 region, the monomer $16_0^2 1_0^1$ appears just to the red of this doublet.[21] It can be seen that the intensity distribution of the dimer features (relative to those of the monomer) does not depend significantly on the detection wavelength, which suggests the absence of excimer formation at this excess energy.

Analogous excimer behavior was observed for clusters produced from isotopic mixtures: $(C_6D_6)_2$ and $(C_6H_6)(C_6D_6)$. Figure 4 shows the fluorescence excitation spectra of a 1:1

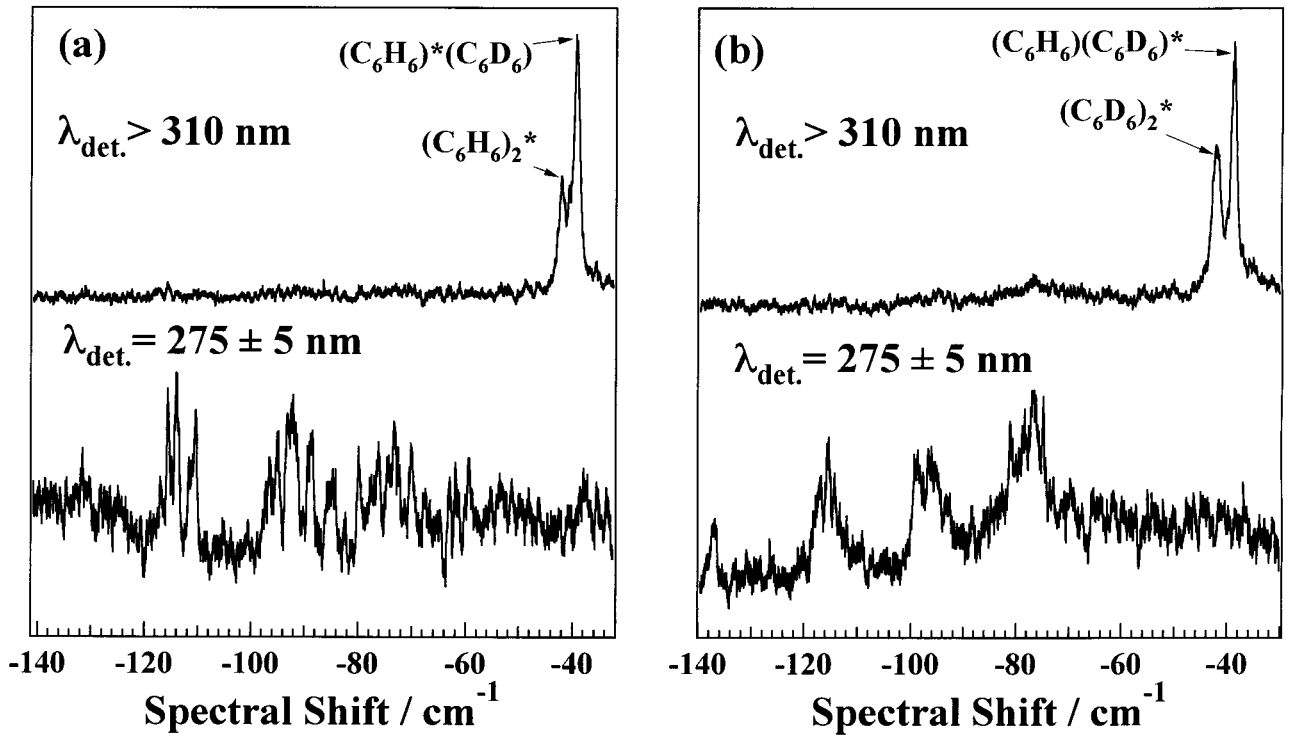

Figure 4. Fluorescence excitation spectra of a 1:1 mixture of C_6H_6 and C_6D_6 near the S_1 origin regions of (a) the $(C_6H_6)_2$ dimer and (b) the $(C_6D_6)_2$ dimer. In each case, fluorescence is detected at >310 nm (top) and 275 ± 5 nm (bottom). The spectral shifts are relative to the respective monomer origins which are separated by 203 cm^{-1}.

mixture of C_6H_6 and C_6D_6 in the S_1 origin regions of $(C_6H_6)_2$ and $(C_6D_6)_2$ dimers, obtained by detecting vdW and excimer fluorescence. The spectral features appearing in the excimer excitation spectra detected at >310 nm [Figure 4 (top)] can be analyzed as a superposition of spectra attributable to pure and mixed dimers, based on comparison with the mass-selective ionization results.[20] To the blue of each origin, one sees a spectral feature whose intensity is approximately two times that of the relevant pure dimer. The one appearing near the $(C_6H_6)_2$ peak [Figure 4a (top)] is assigned to the origin of $(C_6H_6)^*(C_6D_6)$ in which the (C_6H_6) moiety residing in the stem site is excited. The other peak in the vicinity of the $(C_6D_6)_2$ dimer [Figure 4b (top)] corresponds to excitation of a structural isomer with the (C_6D_6) moiety residing in the stem site, i.e., $(C_6H_6)(C_6D_6)^*$. As reported by Börnsen et al.,[20] no splitting is observed for the origins of mixed dimer isotopomers. These origins are absent in the excitation spectrum obtained by detecting fluorescence at 275 nm [Figure 4 (bottom)], which indicates that analogous to the pure dimers, the mixed dimer isotopomers exhibit excimer behavior after 0_0^0 excitation. Moreover, the integrated intensities of the mixed dimer origins are estimated to be nearly identical with those of pure dimer isotopomers if the doublet nature of the latter is taken into consideration. This indicates that the excimer formation efficiency does not depend significantly on isotope substitution.

B. Dispersed Fluorescence Spectra. Dispersed fluorescence spectra were measured after excitation of the 0_0^0, 6_0^1, and $6_0^1 1_0^1$ transitions of the dimer. The spectra of Figure 5 were obtained by exciting the dimer and trimer into their respective origin. Clearly, the two spectra are significantly different from each other. The dimer spectrum (Figure 5a) appears to be broad and significantly red-shifted with respect to that of the trimer (Figure 5b). One also sees that the dimer spectrum reveals sharp features similar to those of the trimer. The structured fluorescence is explained as arising from excitation of the background features (in Figure 1b), which presumably are caused by larger clusters.

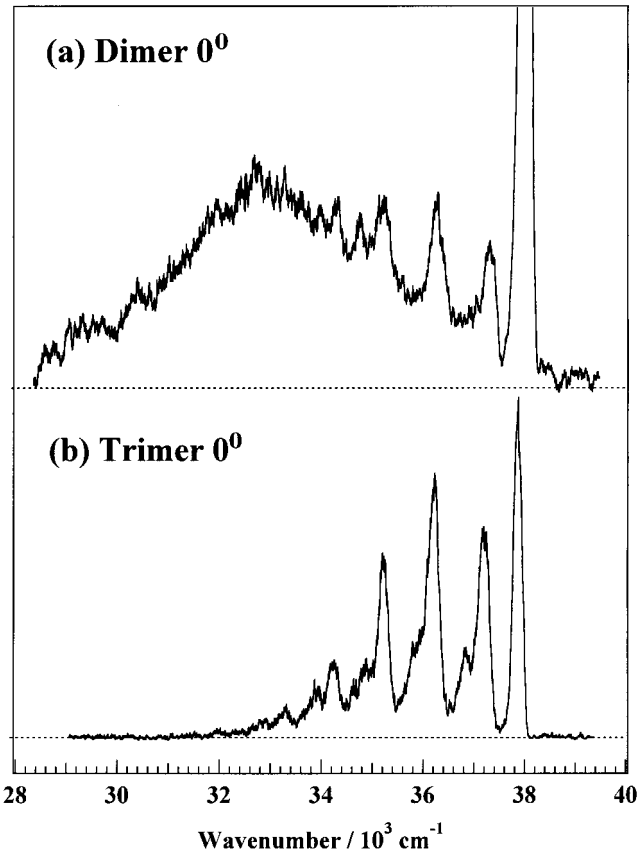

Figure 5. Dispersed fluorescence spectra of (a) the dimer and (b) the trimer, obtained after excitation into the respective 0_0^0 transition. Both spectra are measured with a spectral resolution of 2.5 nm.

The absence of monomer-like fluorescence after the excitation of the dimer is evident based on the observation that the dimer origin does not appear in the excitation spectrum detected at

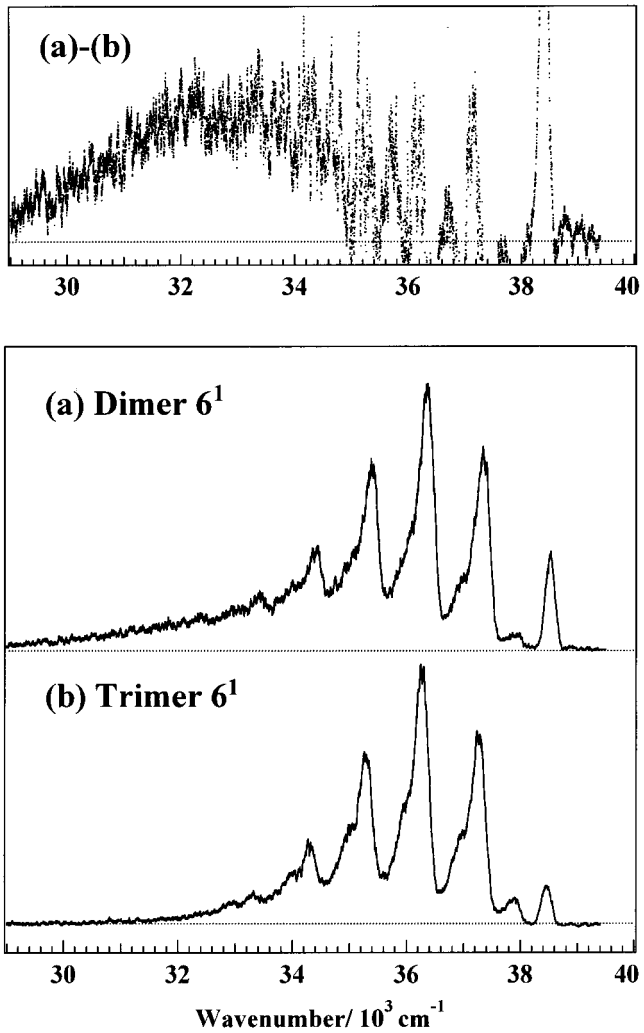

Figure 6. Dispersed fluorescence spectra of (a) the dimer and (b) the trimer, obtained after excitation into the respective 6_0^1 transition. The spectrum in (a) is obtained after excitation of the bluer feature of the dimer doublet at -40 cm^{-1} appearing in Figure 2. Both spectra are measured with a spectral resolution of 2.5 nm. Difference spectrum obtained by subtracting the trimer spectrum in (b) from the dimer spectrum in (a) is shown in the top figure [(a)-(b)].

275 nm (Figure 1b). The intensity maximum of the red-shifted fluorescence is in the wavelength range 305−310 nm, obtained by subtracting the structured fluorescence from the spectrum. We attribute the fluorescence to that of the benzene excimer.

Figure 6 shows the dispersed fluorescence spectra of the dimer and trimer obtained by exciting the relevant 6_0^1 vibronic band. The dimer was excited at the bluer feature of the doublet (Figure 2), because the redder one was found to be superimposed on the monomer 16_0^2 band, as described in section IIIA. Unlike the fluorescence from the dimer origin, the 6^1 fluorescence is dominated by the monomer-like fluorescence which closely resembles that of the trimer. We assign the structured fluorescence to that arising from the vdW geometry. Besides this vdW fluorescence, there is a notable tail, which extends to a longer wavelength than 350 nm. Because such a tail is absent in the trimer spectrum, we assign the red tail of the dimer spectrum to the excimer fluorescence. In fact, the difference spectrum obtained by subtracting the trimer spectrum from that of the dimer, displayed in the top figure of Figure 6, is similar to the excimer fluorescence observed in the origin region. Thus, we conclude that in the 6_0^1 region the dimer emits at both vdW and excimer geometries. Analogous excimer fluorescence was

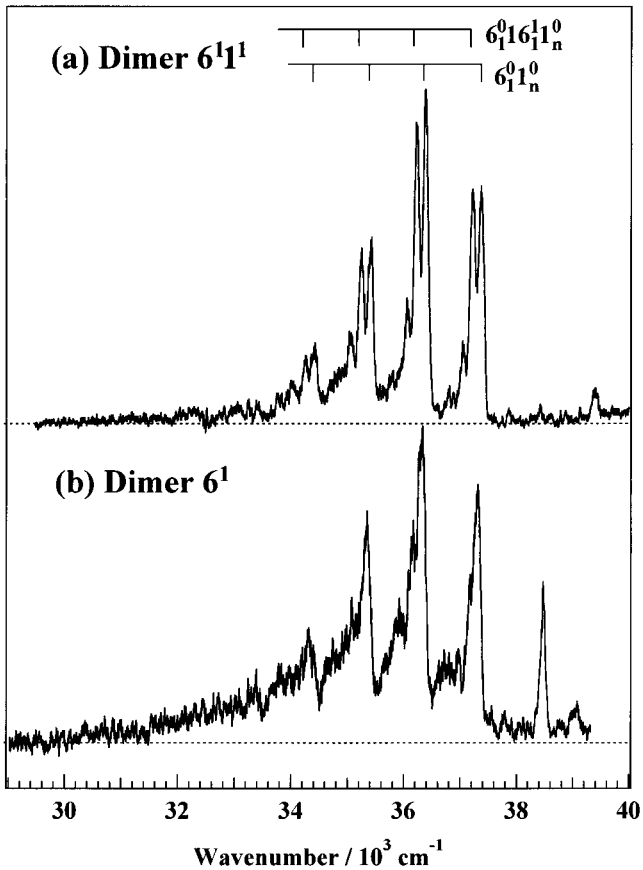

Figure 7. Dispersed fluorescence spectra obtained after excitation of the dimer at (a) the $6_0^1 1_0^1$ transition and (b) the 6_0^1 transition. Both spectra are measured with a spectral resolution of 1.25 nm. The spectrum in (a) is obtained after excitation of the bluer feature of the dimer doublet at -40 cm^{-1} appearing in Figure 3, whereas that in (b) is the same as in Figure 6a except for the spectral resolution.

observed after excitation into the vdW features (namely the top site) of the dimer appearing in Figure 2. The intensity ratio of the excimer fluorescence to the monomer-like fluorescence was virtually the same for the excitation of the stem site and for those of the vdW features.

Figure 7 compares the dispersed fluorescence spectrum obtained by exciting the dimer at the $6_0^1 1_0^1$ doublet (Figure 3) with the 6^1 spectrum measured at a better spectral resolution (1.25 nm) than in Figure 6a. Note the absence of excimer fluorescence in the $6^1 1^1$ spectrum (Figure 7a). Note also the apparent doublet features in the $6^1 1^1$ spectrum. The excess vibrational energy of this excitation is 1444 cm^{-1}, which exceeds the binding energy of this species (560 ± 80 cm^{-1}) determined by Krause et al.[22] Thus, it may be possible that dissociation of the dimer takes place much faster than excimer formation in this region. We therefore tentatively attribute the $6^1 1^1$ fluorescence to monomer fragment fluorescence. On the basis of this assumption, the first peak of each doublet can be assigned to a transition $6_1^0 1_n^0$ ($n = 0, 1, 2, ...$) of the monomer fragment. The splitting of each doublet is approximately 160 cm^{-1}, which matches the difference in the vibrational frequency of ν_{16} between S_1 (237 cm^{-1}) and S_0 (399 cm^{-1}). Thus, we assign the second peak of each doublet to a transition $6_1^0 16_1^1 1_n^0$ ($n = 0, 1, 2, ...$). This assignment implies that a monomer fragment at $S_1 0^0$ or 16^1 is produced upon vibrational predissociation of the dimer.

C. Pump−Probe Fluorescence Depletion Spectroscopy. The benzene excimer in solution exhibits a characteristic absorption in the region 400−575 nm, with an intensity

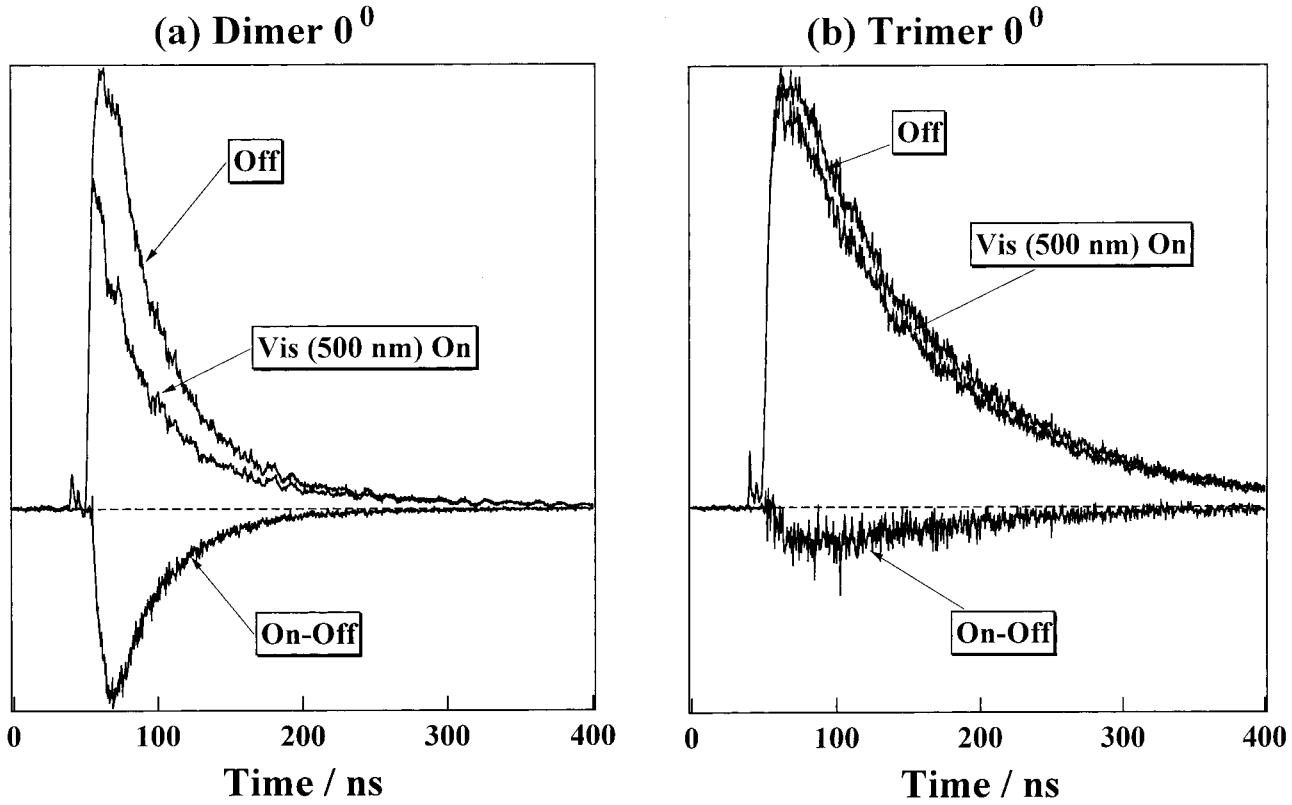

Figure 8. Photodepletion signals for the 0^0 fluorescence of (a) the dimer and (b) the trimer, obtained with a 500-nm probe laser pulse at 0.35 mJ. In both cases, fluorescence is detected through a filter at >270 nm. Difference signal (On−Off) is obtained by subtracting the fluorescence signal generated in the absence of the probe laser irradiation (Off) from that in the presence of the probe laser (On). The time delay between the pump−probe laser pulses is 7 ns.

maximum at 500 nm.[23] At wavelengths longer than 580 nm, the $S_n \leftarrow S_1$ absorption of the monomer dominates. Thus, we have measured fluorescence depletion signals after probe laser irradiation at 500 and 580 nm, to obtain more information on the vdW dimer to excimer dynamics. Figure 8 shows the result obtained with a 500-nm probe pulse at 0.35 mJ, after excitation of the dimer and trimer into their respective S_1 origin. Clearly, two depletion behaviors are significantly different from each other. This difference may be associated with the excimer formation that occurs only in the dimer. The fluorescence depletion magnitude is expressed as $\{I_F(\text{off}) - I_F(\text{on})\}/I_F(\text{off})$, where $I_F(\text{on})$ and $I_F(\text{off})$ are the fluorescence intensities with the probe laser turned on and off, respectively. The value is five times larger for the dimer than for the trimer. This indicates that the excimer produced from the dimer absorbs a 500-nm photon more efficiently than the trimer. In other words, the photodepletion efficiency at 500 nm can be used to measure the extent to which excimer formation occurs.

Figure 9 shows the photodepletion results obtained with a 580-nm probe laser pulse. The pulse energy (0.35 mJ) is the same as in the 500-nm irradiation. In contrast to the strong depletion behavior observed for the dimer at 500 nm, the probe laser irradiation produces no noticeable signal in the dimer fluorescence (Figure 9a). The wavelength-dependent depletion behavior is explained based on the absorption cross-section of the benzene excimer in solution.[23] At 580 nm, only monomer absorbs very weakly, corresponding to the $S_n \leftarrow S_1$ transition. The trimer fluorescence exhibits a weak depletion signal after this irradiation. Similar photodepletion behavior has been observed with a 400-nm probe laser pulse.

Previous photodepletion experiments on excimers on large aromatic molecules[24,25] have revealed that after probe laser irradiation most excimers undergo rapid dissociation into an electronically excited monomer, which gives rise to fragment fluorescence, and a ground-state monomer. This results in the appearance of monomer fluorescence while generating the depletion in excimer fluorescence intensity. Figure 10 shows the results of such an experiment on the 0^0 fluorescence of the benzene dimer. The 500-nm irradiation does not lead to an increase in fluorescence intensity when detected at 275 nm (Figure 10a). The 275-nm fluorescence obtained in the absence of the probe laser pulse, which corresponds to the structured fluorescence appearing in Figure 5a, arises from excitation of higher-order clusters. Thus, the depletion magnitude of this fluorescence is exhibited to be similar to that observed for the trimer 0^0 fluorescence. We therefore conclude that the 500-nm irradiation does not produce any monomer fragment that emits at 275 nm. In contrast, strong depletion is present for the excimer fluorescence detected at >310 nm (Figure 10b).

Figure 11 shows photodepletion behaviors of the 6^1 dimer obtained by irradiation at 500 nm while monitoring the vdW fluorescence at 275 nm and the excimer fluorescence at >310 nm. The depletion magnitude is essentially the same for each fluorescence (≈0.41), which is noticeably smaller than that of the 0^0 fluorescence (≈0.68 in Figure 10b). This point is particularly important in elucidating the dynamics of excimer formation, as discussed in section IVA. Figure 12 displays such excitation energy dependence of depletion behavior. Total fluorescence intensity (>270 nm) was detected for each excitation. It is evident that the depletion magnitude decreases with increasing excess energy. The depletion yield of the fluorescence from the $6^1 1^1$ level (Figure 12c) is much lower than those of the 0^0 and 6^1 levels. This is expected given that this fluorescence arises from a monomer fragment after vibrational predissociation which takes place much faster than excimer formation.

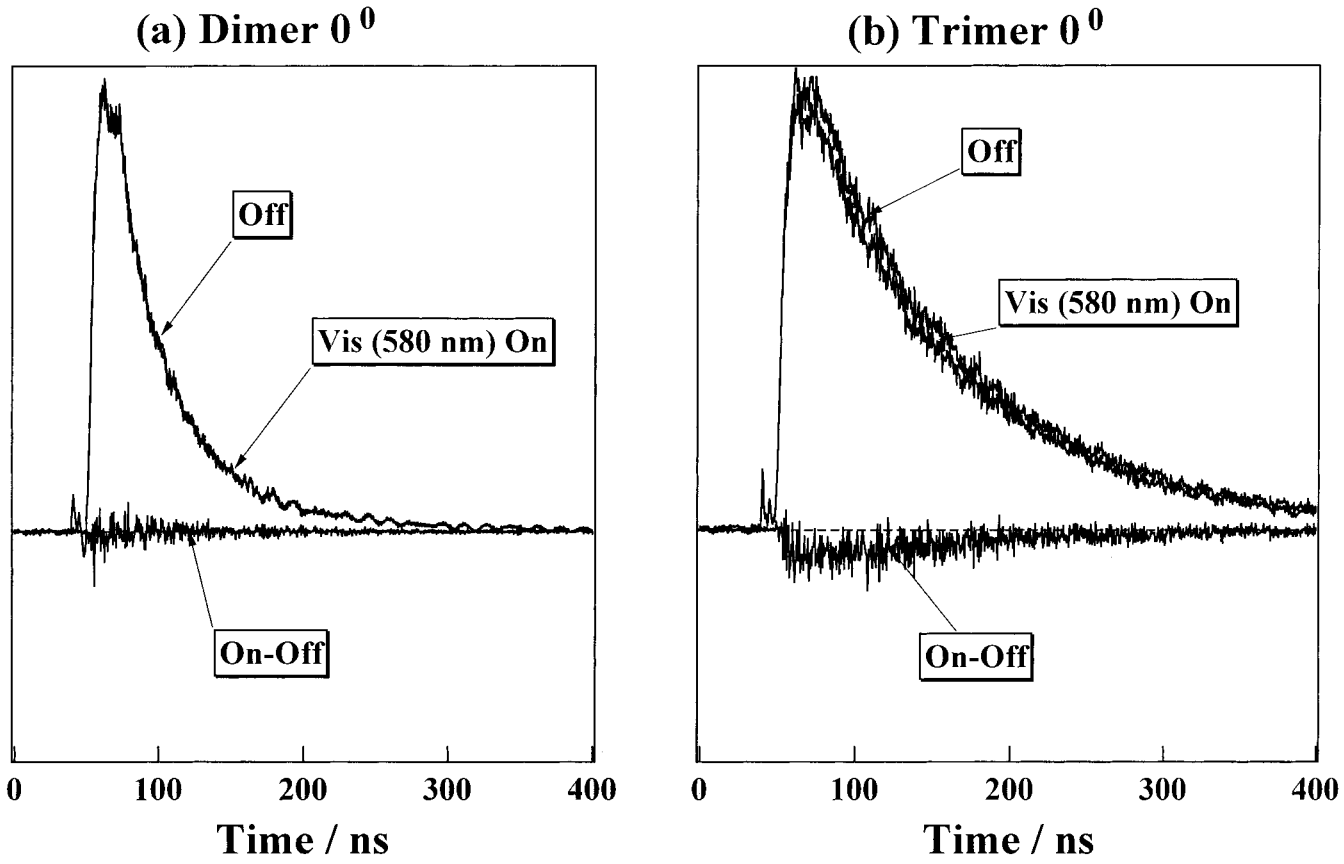

Figure 9. Photodepletion signals for the 0^0 fluorescence of (a) the dimer and (b) the trimer, obtained with a 580-nm probe laser pulse (0.35 mJ). In both cases, fluorescence is detected at >270 nm.

D. Fluorescence Lifetimes. Previous two-color photoionization results[9] suggested that the 0^0 and 6^1 lifetimes of the benzene dimer are 36 and 40 ns, respectively, which are shorter than the respective monomer lifetimes (103 and 82 ns). The shortening of the dimer lifetimes was attributed to excimer formation. However, the present fluorescence results clearly demonstrate that the lifetimes obtained by the ionization method are actually those of the excimers, because the excimer fluorescence lifetimes (39 ns for 0^0 and 46 ns for 6^1) match well the ionization results. As mentioned above, the vdW fluorescence lifetime is identical with the excimer lifetime, suggesting the existence of a dimer−excimer equilibrium upon excitation into the 6^1_0 level. In contrast, the 6^11^1 fluorescence lifetime (69 ns) may be associated with that of a monomer fragment produced upon predissociation. The lifetimes of the dimer and trimer are listed in Table 1.

IV. Discussion

A. Dynamics of Excimer Formation. The present results demonstrate unequivocally the occurrence of excimer formation upon excitation of the T-shaped benzene dimer into its S_1 electronic origin and 6^1_0 band. The evidence is the appearance of broad, red-shifted fluorescence which is characteristic of the benzene excimer in solution. Such excimer behavior is absent in the trimer and tetramer. The dimer also exhibits an interesting excitation energy-dependent behavior. Although it gives rise to only excimer fluorescence after 0^0_0 excitation, both vdW and excimer fluorescence are observed at the 6^1 level. Moreover, the dimer is likely to dissociate into monomer fragments at the 6^11^1 level. This behavior is apparently different from those of naphthalene trimer and tetramer,[26] in which excimer formation requires a certain amount of energy to surmount an activation barrier and its efficiency increases with increasing excess energy.

The 0^0 Region. The occurrence of excimer formation without requiring any excess vibrational energy can be taken as evidence that the dynamics is a tunneling-induced isomerization process. The S_1 origin of the benzene dimer $(C_6H_6)_2$ exhibited a doublet with 1.7 cm^{-1} splitting (1.5 cm^{-1} in Figure 1a), which is absent on the origin of the mixed dimer isotopomers (Figure 4).[20] The splitting was attributed to an excitation exchange (exciton) interaction by invoking a dimer of two equivalent sites. On the basis of the T-shaped geometry, however, Henson et al.[1] argued that such splitting could arise from a site-exchange interaction between two inequivalent sites. Given that the excimer state exists below the T-shaped dimer state and they interact with each other, it is tempting to explain the homodimer's splitting by tunneling between the two excited states. This possibility has been ruled out based on the observation that the heterodimer isotopomers also exhibit excimer fluorescence after 0^0_0 excitation [Figure 4 (top)]. Excimer formation would not be expected for the heterodimers because their origin bands show no such splitting. Analogous isotopomer-independent behavior has been observed in the fluorene dimers.[27] Whereas the 0^0_0 band of the pure dimer $(C_{13}H_{10})_2$ exhibits complicated spectral features which can be associated with exciton splitting coupled with intermolecular vibrational modes, the heterodimer's origin is characterized by a simple progression in an intermolecular vibration. Nonetheless, both species undergo excimer formation with high efficiency. Thus, there is no manifestation at present that the splitting of the benzene homodimer is caused by tunneling between the dimer and excimer states. Besides the splitting, the 0^0_0 band appearing in the excimer excitation

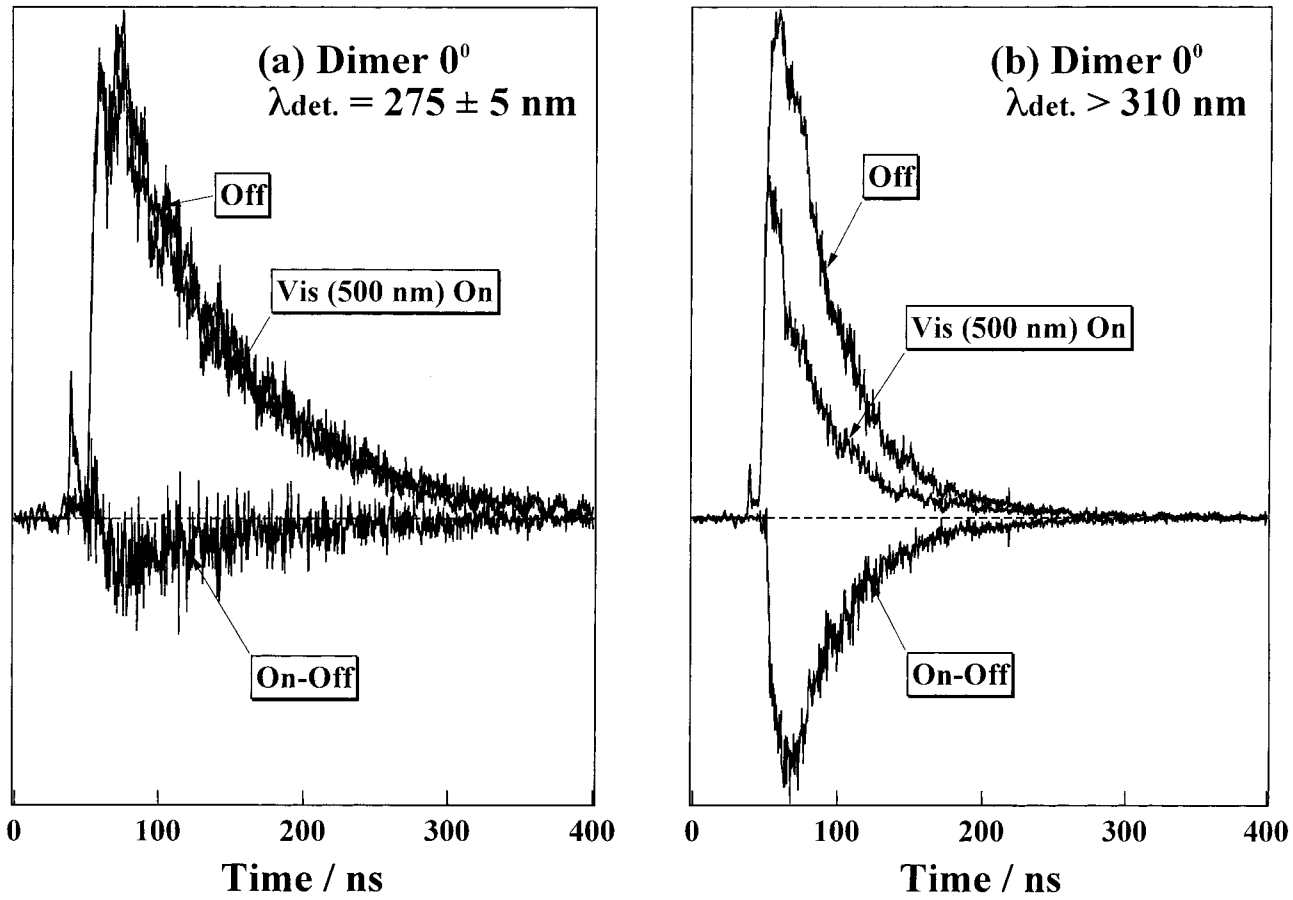

Figure 10. Photodepletion signals obtained with a 500-nm probe pulse (0.35 mJ) for the fluorescence generated by the pump laser set to the dimer 0_0^0 transition and detected (a) at 275 ± 5 nm and (b) at >310 nm. The fluorescence in (a) is assigned as arising from large benzene clusters, and that in (b) is due to the benzene excimer.

spectrum of Figure 1a exhibits a distinct broadening compared with those of the trimer and tetramer (Figure 1b). The width of each band of the splitting, which is evaluated by deconvolution to be ≈1.2 cm^{-1} full width at half-height, may be associated with unresolved rotational structure.

The 6^1 Region. Unlike the total conversion of the 0^0 dimer into the excimer, the excimer produced at the 6^1 level maintains an equilibrium with the vdW dimer before relaxation to the ground state. Thus, we adopt the following scheme to explain the excimer formation kinetics in the 6^1 region:

$$\begin{array}{ccc} [D_0] & \underset{k_{ED}}{\overset{k_{DE}}{\rightleftharpoons}} & [E_0] \\ \downarrow k_{DG} & & \downarrow k_{EG} \end{array}$$

$[D_0]$ and $[E_0]$ refer to the dimer and excimer states, and k_{DE} and k_{ED} are the excimer formation and dissociation (back-reaction) rate constants. Both states decay to the ground state by the rate constants k_{DG} and k_{EG}. The assumption of rapid equilibrium is borne out by essentially the same depletion yield for the vdW and excimer fluorescence (Figure 11), which is also consistent with the observation that the two types of fluorescence have the same single-exponential lifetime (≈46 ns in Table 1). This behavior corresponds to the high-temperature limit (dynamic equilibrium) proposed to explain the excimer dynamics in solution (i.e., k_{DE}, $k_{ED} \gg k_{DG}$, k_{EG}).[28] Under this condition, we can estimate the equilibrium constant $K_{eq} = [E_0]/[D_0] = k_{DE}/k_{ED}$ based on the results of photodepletion.

The photodepletion magnitudes of the vdW dimer and excimer fluorescence are given by

$$\Delta I_F^D = \frac{I_F^D(\text{off}) - I_F^D(\text{on})}{I_F^D(\text{off})} = \frac{[D_0] - [D]}{[D_0]} \quad (1)$$

$$\Delta I_F^E = \frac{I_F^E(\text{off}) - I_F^E(\text{on})}{I_F^E(\text{off})} = \frac{[E_0] - [E]}{[E_0]} \quad (2)$$

respectively, where $I_F(\text{on})$ and $I_F(\text{off})$ are the fluorescence intensities when the visible laser is turned on and off, respectively, and $[D]$ and $[E]$ represent respective populations attained after photodepletion. Thus, the observed depletion for the 6^1 fluorescence may be given by the relation

$$\Delta I_F(6^1) = \frac{[D_0] + [E_0] - \{[D] + [E]\}}{[D_0] + [E_0]} = \frac{\Delta I_F^D[D_0] + \Delta I_F^E[E_0]}{[D_0] + [E_0]} \quad (3)$$

From eq 3 we obtain the equilibrium constant

$$K_{eq}(6^1) = \frac{[E_0]}{[D_0]} = \frac{\Delta I_F(6^1) - \Delta I_F^D}{\Delta I_F^E - \Delta I_F(6^1)} \quad (4)$$

To evaluate $K_{eq}(6^1)$, we assume that the vdW fluorescence depletion ΔI_F^D of the dimer is the same as that of the trimer (≈0.1) because the trimer does not form excimer. Using the observed depletion magnitudes of ΔI_F^E (0.68 for the 0^0 fluorescence) and $\Delta I_F(6^1)$ (0.41), we observe that $K_{eq}(6^1) \approx 1.1$. This indicates that the equilibrium populations of the vdW dimer and excimer are almost identical.

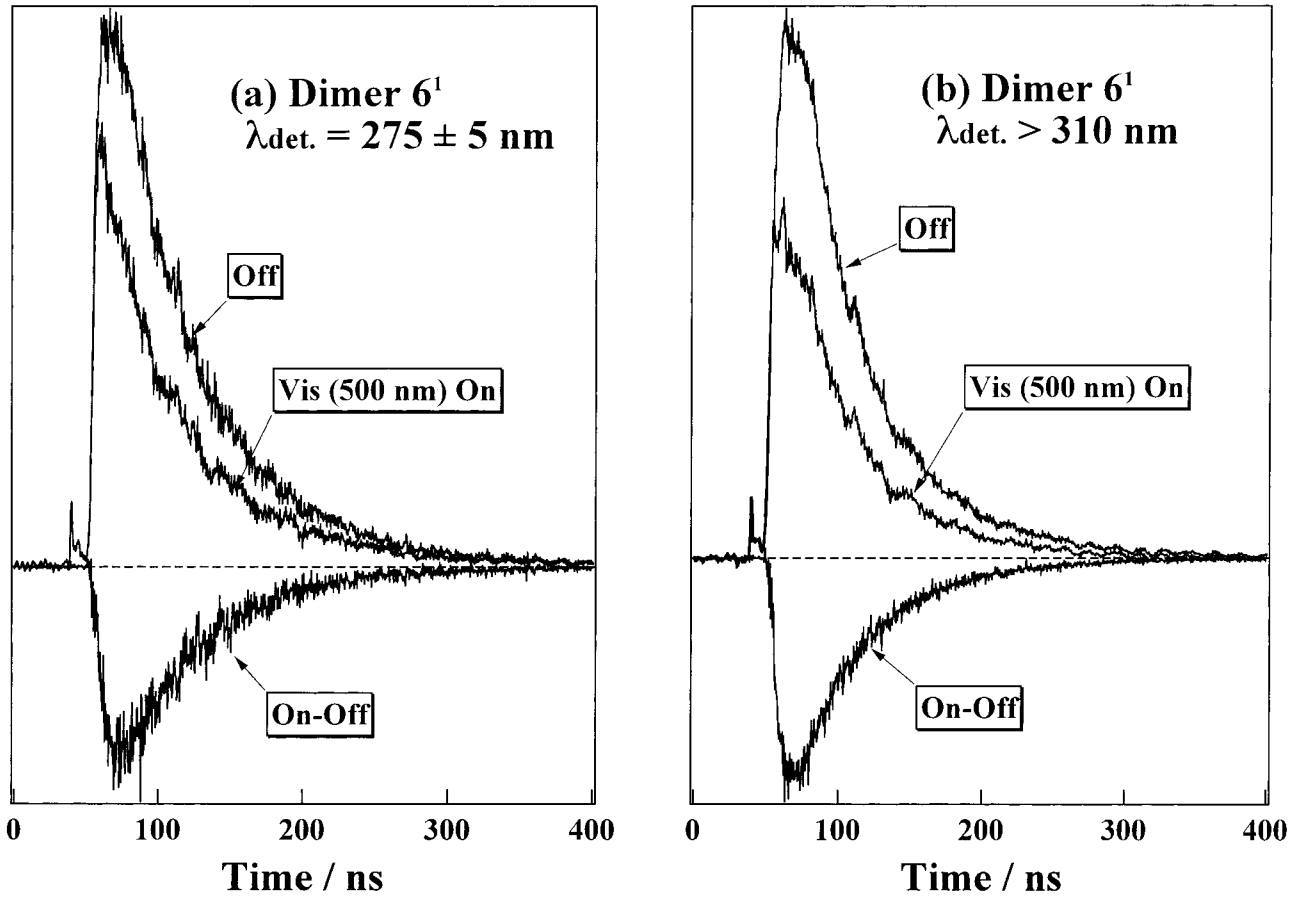

Figure 11. Photodepletion signals with a 500-nm probe pulse (0.35 mJ) for the dimer 6^1 fluorescence detected (a) at 275 ± 5 nm and (b) at >310 nm. The pump laser beam is set to the bluer feature of the doublet in Figure 2.

Next, we consider the relative quantum yields for the vdW-type and excimer fluorescence obtained after 6_0^1 excitation, which is given by

$$\frac{\Phi_{EG}}{\Phi_{DG}} = \frac{k^r_{EG}}{k^r_{DG}} \frac{[E_0]}{[D_0]} \tag{5}$$

where k^r_{DG} and k^r_{EG} are the radiative decay rate constants for the dimer and excimer, respectively. The ratio Φ_{EG}/Φ_{DG} is obtained experimentally by dividing the integrated intensity of the excimer fluorescence by that of the vdW-type fluorescence. This yields $\Phi_{EG}/\Phi_{DG} \approx 0.27$ based on the results in Figure 6. With use of the values of $K_{eq}(6^1)$ and Φ_{EG}/Φ_{DG}, the relative radiative decay constant $k^r_{EG}/k^r_{DG} \approx 0.25$. Thus, the low fluorescence yield of the excimer produced from the 6^1 level may be associated with the small radiative rate constant.

Finally, one must consider why the excimer back-reaction into the vdW dimer occurs efficiently at the 6^1 level ($K_{eq}(6^1) = k_{DE}/k_{ED} \approx 1.1$). Such an equilibrium behavior is absent at the 0^0 level and thus no vdW-type fluorescence is observed. This difference is attributable to the 521 cm^{-1} of excess energy. At this excess energy, the density of low-frequency vdW modes of the T-shaped potential well is expected be quite high. Moreover, the 6^1 level is located near the dissociation threshold of the dimer, which may render the T-shaped structure very floppy. These vdW modes should consist of a set of reactive modes, which lead to excimer formation, and numerous of nonreactive modes, which produce vdW fluorescence. When the structure becomes less rigid, the two sets of vdW modes will mix extensively with each other. In this case, a large distribution of vdW states can interact with excimer states, thus ensuring that an equilibrium is maintained. As a result, the overall excimer formation may become less efficient and reversible. This reversible behavior corresponds well to the high-temperature kinetics, which, in fact, has been proposed for the benzene excimer formation in solution.[29] For the 0^0 level, on the other hand, the initially excited single level must interact directly with a set of isoenergetic excimer levels via tunneling, and thus the dynamics becomes irreversible.

The $6^1 1^1$ Region. No excimer behavior is observed in this region, in contrast to the 0^0 and 6^1 results. This is to be expected because the dimer undergoes rapid vibrational predissociation in this excess energy range (1444 cm^{-1}). This energy is significantly greater than the dissociation energy of the benzene dimer (560 cm^{-1}).[22] The absence of photodepletion signal on the fluorescence in this region is also consistent with this interpretation. This behavior is in contrast to other aromatic dimers in which excimer formation always occurs more quickly than predissociation. This difference may be explained by a geometrical factor that influences the excimer formation dynamics, and will be discussed below.

B. Structure and Stability of the Benzene Excimer. Experimental information available on the structures of aromatic excimers is incomplete. Thus, most theoretical calculations[30,31] have been made only on highest symmetry, namely, that excimer geometry in which one of the monomers is superimposed exactly above the plane of the other. The stability is usually explained by configuration interactions of exciton-resonance states ($\phi^*\phi \pm \phi\phi^*$) and charge-resonance states ($\phi^+\phi^- \pm \phi^-\phi^+$). Important information regarding the structure of benzene excimer is the observation of strong two-color ionization signals of the dimer

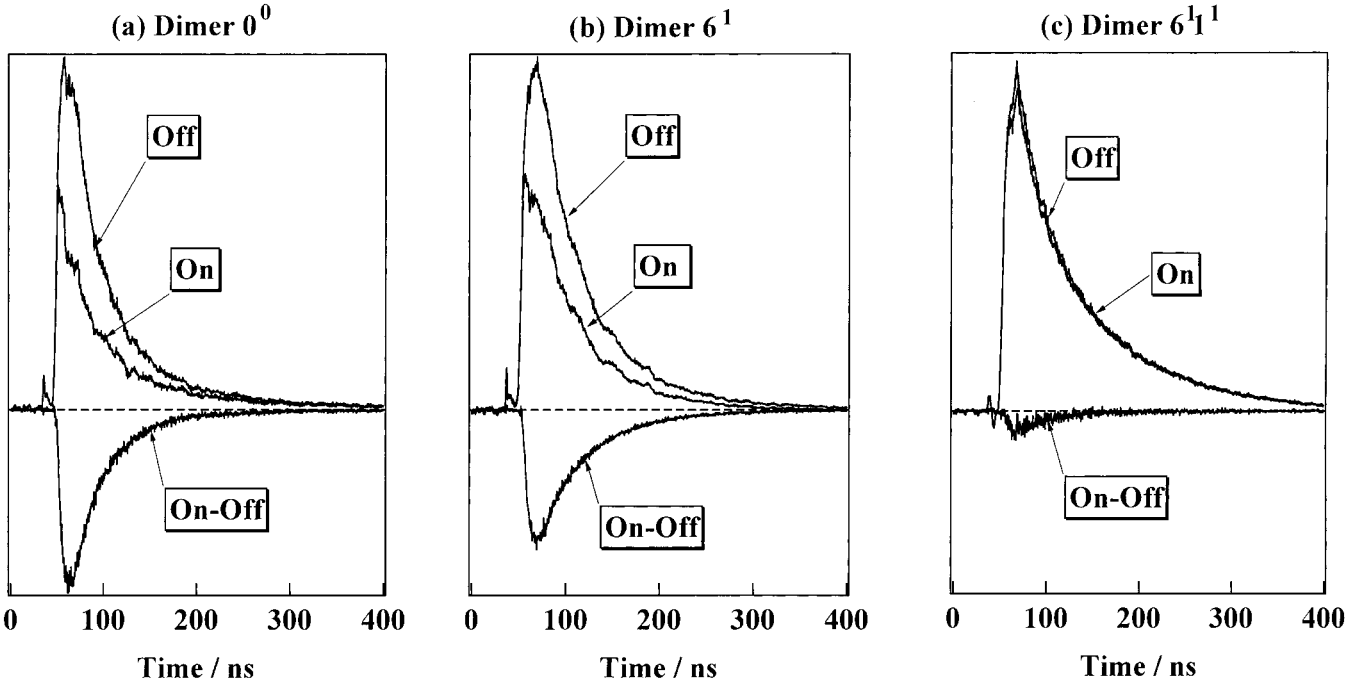

Figure 12. Comparison of photodepletion signals obtained with a 500-nm probe pulse (0.35 mJ) for the fluorescence from (a) 0^0, (b) 6^1, and (c) $6^1 1^1$ levels of the dimer. In all cases, total fluorescence intensity (at >270 nm) is detected through a filter. In (b) and (c), the pump laser beam is set to the bluer feature of the respective doublet in Figures 2 and 3.

TABLE 1: Comparison of the S_1 Lifetimes of the Dimer and Trimer[a]

S_1 levels	dimer (vdW)	dimer (excimer)	trimer
0^0		39	76
6^1	46,[b] 52[c]	46,[b] 51[c]	106
$6^1 1^1$	69[d]		

[a] All lifetimes are in nanoseconds. [b] The values obtained subsequent to excitation into the bluer feature of the stem site. [c] The values obtained subsequent to excitation into the vdW feature of the top site appearing at +12 cm^{-1} in Figure 2. [d] The value for the monomer fragment fluorescence.

cation $(C_6H_6)_2^+$ when the dimer is ionized via intermediate S_1 levels.[9] This ionization enhancement (compared with the trimer) is explained by invoking an excimer structure that is similar to that of $(C_6H_6)_2^+$. Because the dimer cation is likely to be stabilized by a charge-resonance interaction ($\phi^+\phi \leftrightarrow \phi\phi^+$), its structure may resemble that of the excimer. This structural similarity was associated with the higher ionization cross-section for the dimer (via excimer formation) than for the trimer.[9] For the dimer cation, Ohashi and Nishi[32] proposed a parallel geometry to account for the observation of a charge-resonance absorption band in the near-IR region. Such structure is in good agreement with the most recent theoretical result by Miyoshi et al.[33] Given this structure, one would expect that the excimer also have a similar parallel structure.

Such a parallel excimer geometry is apparently different from the T-shaped geometry of the vdW dimer. How can it account for the present results on the excimer dynamics? Our fluorescence results show that there is a steric barrier which isolates the initially prepared vdW state from the fluorescent excimer state. These two states interact only weakly with each other through a set of intermolecular coordinates (weak coupling). If we consider only one coordinate, the angle between the two benzene rings (0° for parallel and 90° for T-shaped), then the excimer formation occurs via tunneling through this coordinate. In this case, the absorption profile of the 0_0^0 band is expected to be broadened only by tunneling and, in fact, a simple, relatively sharp (≈2 cm^{-1}) feature corresponding to the S_1 origin is observed.

If the excimer possessed a similar T-shaped geometry, the formation coordinate would primarily be a one-dimensional motion of two benzene sites, thus resulting in a reactive potential without barrier. This would give rise to broad, complicated absorption bands caused by a strong interaction of the two states. Such a strong coupling behavior is, in fact, observed for dimers of large aromatic molecules (e.g., naphthalene,[26] fluorene,[17,18] and anthracene[34]), in which excimer formation occurs on the picosecond time scale (≈36 ps for the fluorene dimer[35]). Moreover, $S_1 \leftarrow S_0$ excitation spectra of these dimer systems are characterized by complicated spectral features probably caused by coupling with intermolecular vibrations (e.g., fluorene[27]) or by unresolved broad bands (e.g., naphthalene,[26] pyrene[36]). The vastly different spectral shapes (sharp vs broad) may be taken as evidence of a structural difference between the benzene dimer, which is T-shaped, and other large aromatic dimers. Consistent with this conjecture, theoretical[37] and experimental[38] results suggest that for complexes involving large aromatic molecules, the dispersion interaction favors parallel (stacked) over nonparallel (T- or V-shaped) geometries.

Another striking difference between benzene and large aromatic dimers is the excitation energy dependence of excimer formation. Whereas, in the benzene dimer, the dynamics occurs only near the bottom of the vdW well (i.e., at 0^0 and 6^1), excimer formation in other dimers is independent of excitation energy. The absence of noticeable excitation energy dependence may be expected if vdW and excimer states mix strongly with each other because of structural similarity. This is also consistent with the observation that vibrational predissociation, which is observed for $6^1 1^1$ of the benzene dimer, does not significantly compete with excimer formation in large aromatic dimers.

The stability of benzene excimer has been the important subject of calculations. Birks[28] proposed that charge-resonance

interaction dominates and the excimer may be formed in a variety of nonsandwiched configurations. Based on the D_{6h} structure, Vala et al.[31] attributed the lowest excimer state to an exciton-resonance state that correlates to the S_1 state of the monomer whereas they explained its stability by an interaction with a charge-transfer state located at a higher energy. In this approximation, the energy of the lowest excimer state depends on both the interplanar separation and the energy of the charge-transfer state. Although the location of the charge-transfer state is not known, it is estimated to be 5.9 eV above the monomer S_1 state (4.72 eV) at infinite separation, based on the ionization potential (9.24 eV) and electron affinity (-1.4 eV[39]) of benzene. Such a charge-transfer state may be lowered as the two benzene moieties come closer together, thus explaining the excimer stability. The observed red shift of the excimer fluorescence was reproduced based on an excimer with an interplanar separation of $\approx$3 Å. However, this model cannot readily explain the 500-nm absorption band of the excimer.

Excimers of large aromatic molecules (e.g., naphthalene[24] and fluorene[25]) exhibit an absorption band in the near-IR region. The strong absorption was assigned to the intervalence transition from the lowest exciton state ($\phi^*\phi - \phi\phi^*$) to the upper exciton state ($\phi^*\phi + \phi\phi^*$) of repulsive character, both stabilized by configuration interactions with a charge-transfer state.[24] For the benzene excimer of D_{6h} symmetry, however, this approximation gives rise to an energy separation of $\approx$3000 cm^{-1} between the lowest (B_{1g}) and upper (B_{2u}) exciton components, both originating in the monomer S_1 (B_{2u}) state.[31] Apparently, the small splitting cannot account for the observed 500-nm band of the benzene excimer. Based on this energy-gap consideration, the upper excimer state arising from the 500-nm absorption was previously assigned to the excimer state E_{1u} that correlates to the monomer E_{1u} state.[40] This assignment yields a $\Delta E(E_{1u} - B_{1g})$ of 2.4 eV.[31]

It may also be possible to assign the excimer absorption band to the transition from the lowest excimer state to the charge-transfer state that correlates to $(C_6H_6)^+ + (C_6H_6)^-$. In this case, the lowest excimer state must be of charge-transfer character to explain the large absorption cross-section for this transition. Moreover, such a *charge-transfer complex* will not dissociate into neutral monomer fragments upon photoexcitation at 500 nm, thus explaining the absence of monomer fluorescence. The importance of the charge-transfer state in the stabilization of the benzene excimer is also in agreement with the observed fluorescence red-shift. Similar conclusion has recently been reached for other aromatic excimers involving fluorene.[41]

V. Conclusions

Direct evidence of the excimer formation has been obtained by exciting the T-shaped benzene dimer into its S_1 levels and by observing excimer fluorescence. Based on the results of the photodepletion experiments with fluorescence detection, it is demonstrated that the dynamics occurs much faster than the respective decay processes to the ground state. Although at the S_1 origin the excimer formation proceeds via tunneling between the equilibrium geometries of the T-shaped dimer and excimer, an excimer back-reaction into the dimer occurs as quickly as the excimer formation at the 6^1 level (521 cm^{-1} excess energy), thus leading to an equilibrium between these two states. Further increase in excitation energy results in vibrational predissociation of the dimer. These dynamics are quite different from those observed for dimers of larger aromatic molecules. The T-shaped geometry, which is very different from a parallel stacked geometry assumed for the excimer, is inferred to be an important factor influencing the benzene-dimer dynamics. This geometry difference renders the energy barrier relatively high and the excimer formation coordinate more restricted than in other aromatic dimers.

Acknowledgment. This work was supported in part by a research fund provided by Yokohama City University. We would like to thank Professor K. Kojima for the loan of the monochromator and Professor Y. Nishimura for the use of his equipment, both of which made these experiments possible. We also thank Professors N. Nishi and D. H. Levy for helpful discussions.

References and Notes

(1) Henson, B. T.; Hartland, G. V.; Venturo, V. A.; Felker, P. M. *J. Chem. Phys.* **1992**, *97*, 2189.
(2) Arunan, E.; Gutowsky, H. S. *J. Chem. Phys.* **1993**, *98*, 4294.
(3) Hobza, P.; Selzle, H. L.; Schlag, E. W. *J. Chem. Phys.* **1990**, *93*, 5893.
(4) Hobza, P.; Selzle, H. L.; Schlag, E. W. *J. Phys. Chem.* **1993**, *97*, 3937.
(5) Tsuzuki, S.; Uchimaru, T.; Tanabe, K. *J. Mol. Struct. THEOCHEM.* **1994**, *307*, 107.
(6) Jaffe, R. L.; Smith, G. D. *J. Chem Phys.* **1996**, *105*, 2780.
(7) Li, Z. Q.; Ohno, K.; Kawazoe, Y. *Surf. Rev. Lett.* **1996**, *3*, 359.
(8) Chipot, C.; Jaffe, R.; Maigret, B.; Pearlman, D. A.; Kollman, P. A. *J. Am. Chem. Soc.* **1996**, *118*, 11217.
(9) Hopkins, J. B.; Powers, D. E.; Smalley, R. E. *J. Phys. Chem.* **1981**, *85*, 3739.
(10) Law, K. S.; Schauer, M.; Bernstein, E. R. *J. Chem. Phys.* **1984**, *81*, 4871.
(11) Langridge-Smith, P. R. R.; Brumbaugh, D. V.; Haynam, C. A.; Levy, D. H. *J. Phys. Chem.* **1981**, *85*, 3742.
(12) Krätzschmar, O.; Selzle, H. L.; Schlag, E. W. *J. Phys. Chem.* **1994**, *98*, 3501.
(13) Shinohara, H.; Nishi, N. *J. Chem. Phys.* **1989**, *91*, 6743.
(14) Ernstberger, B. Ph.D. Thesis, Technische Universität Munchen, 1991.
(15) Radloff, W.; Freudenberg, Th.; Ritze, H.-H.; Stert, V.; Noack, F.; Hertel, I. V. *Chem. Phys. Lett.* **1996**, *261*, 301.
(16) Saigusa, H.; Lim, E. C. *Acc. Chem. Res.* **1996**, *29*, 171.
(17) Saigusa, H.; Itoh, M. *J. Phys. Chem.* **1985**, *89*, 5486.
(18) Saigusa, H.; Lim, E. C. *J. Phys. Chem.* **1991**, *95*, 2364.
(19) Birks, J. B.; Braga, C. L.; Lumb, M. D. *Proc. R. Soc. London, Ser. A* **1965**, *283*, 1965.
(20) Börnsen, K. O.; Selzle, H. L.; Schlag, E. W. *J. Chem. Phys.* **1986**, *85*, 1726.
(21) Stephenson, T. A.; Radloff, R. L.; Rice, S. A. *J. Chem. Phys.* **1984**, *81*, 1060.
(22) Krause, H.; Ernstberger, B.; Neusser, H. J. *Chem. Phys. Lett.* **1991**, *184*, 411.
(23) Nakashima, N.; Sumitani, M.; Ohmine, I.; Yoshihara, K. *J. Chem Phys.* **1980**, *72*, 2226.
(24) Saigusa, H.; Sun, S.; Lim, E. C. *J. Phys. Chem.* **1992**, *96*, 10099.
(25) Sun, S.; Saigusa, H.; Lim, E. C. *J. Phys. Chem.* **1993**, *97*, 11635.
(26) Saigusa, H.; Sun, S.; Lim, E. C. *J. Phys. Chem.* **1992**, *96*, 2083.
(27) Saigusa, H.; Sun, S.; Lim, E. C. *J. Phys. Chem.* **1992**, *95*, 1194.
(28) Birks, J. B. *Photophysics of Aromatic Molecules*; Wiley: New York, 1970; Chapter 7.
(29) Cundall, R. B.; Robinson, D. A. *J. Chem Soc., Faraday Trans. 2* **1973**, *18*, 371.
(30) Srinivasan, B. N.; Russell, J. V.; McGlynn, S. P. *J. Chem. Phys.* **1968**, *48*, 1931.
(31) Vala, M. T.; Hillier, I. H.; Rice, S. A.; Jortner, J. *J. Chem Phys.* **1966**, *44*, 23.
(32) Ohashi, K.; Nishi, N. *J. Chem. Phys.* **1991**, *95*, 4002.
(33) Miyoshi, E.; Ichikawa, T.; Sumi, T.; Sakai, Y.; Shida, N. *Chem. Phys. Lett.* **1997**, *275*, 404.
(34) Charkraborty, T.; Lim, E. C. *J. Phys. Chem.* **1993**, *97*, 11151.
(35) Saigusa, H. To be submitted for publication.
(36) Suzuka, I. To be submitted for publication.
(37) Jorgensen, W. L.; Severance, D. L. *J. Am. Chem. Soc.* **1990**, *112*, 4768.
(38) Joireman, P. W.; Connell, L. L.; Ohline, S. M.; Felker, P. M. *J. Phys. Chem.* **1991**, *95*, 4935.
(39) Pope, M.; Swenberg, C. E. *Electronic Processes in Organic Crystals*; Clarendon: Oxford: 1982; p 204.
(40) Cooper, R.; Thomas, J. K. *J. Chem. Phys.* **1968**, *48*, 5097.
(41) Yip, W. T.; Levy, D. H. *J. Phys. Chem.* **1996**, *100*, 11539.